J Electroceram (2008) 20:65–71
DOI 10.1007/s10832-007-9345-6

Low temperature hydrothermal routes to various PZT stoichiometries

Scott Harada · Steve Dunn

Received: 30 April 2007 / Accepted: 10 October 2007 / Published online: 13 November 2007

Abstract The production of lead zirconate titanate (PZT) with a variation in Zr and Ti ratios using a hydrothermal method has been attempted. We show that when reactions are conducted at 160 °C, for 4 h, the phase of PZT produced is independent of the initial Zr/Ti precursor ratio. In all cases we produce PZT with a crystal structure close to the morphotropic phase boundary, i.e. Zr/Ti≈52:48. The excess precursors either fail to react, or form amorphous and crystalline impurity phases that are detectable via powder XRD after the hydrothermal treatment. Using an excess of Pb precursor is shown to aid the crystallisation of the resultant PZT powder, as verified by SEM and FIB analysis.

Keywords Hydrothermal synthesis · PZT · Zirconium-titanium ratios · Microstructure

1 Introduction

In recent years there has been an increasing desire to develop and manufacture microelectromechanical systems (MEMS). These systems can possess significant benefits over their macroscopic counterparts, such as reduced power consumption and form-factor and increased robustness. One of the key material types that is being developed for MEMS applications are the ferroelectrics whose properties such as high dielectric constants and domain polarisation [1] have led to a wide range of interesting and diverse applications. Amongst the ferroelectric materials, the use of the solid solution lead zirconate titanate (PZT) has become widespread due to its high d_{33} and electromechanical coupling. In order to make the most out of MEMS devices it is important to produce the PZT on, in the main, silicon substrates. This has been the case for the incorporation of microelectronics and for compatibility with the existing silicon micromanufacturing techniques and understanding. This has posed a number of problems due to the low softening temperature of silicon and the relatively high processing temperature of PZT. In order to overcome these problems, several techniques have been developed that aim to reduce the temperature at which the ferroelectric PZT phase crystallises [2]. These include sol-gel, coprecipitation and hydrothermal synthesis. When dealing with PZT intrinsic material properties such as the electromechanical coupling vary with Zr/Ti ratio and processing conditions. It is therefore possible to modify the behaviour of PZT by changing the stoichiometry of the final ceramic. However, varying the Zr/Ti ratio in precursor materials does not lead to simple changes in the final product.

The initial problems with sol-gel producing inhomogeneous films, for example [3], have now largely been solved [4, 5]. The use of the hydrothermal technique to produce thin films of PZT on substrates has some advantages over sol-gel and sputtering in that curved surfaces can be coated [6–8] and a variety of substrate materials can be used [9]. During the development of the hydrothermal technique there existed a variety of techniques for the synthesis of PZT with initial studies producing a mixture of lead titanate and lead zirconate. Through an investigation of the relative solubility of the precursor material [10] some indications as

S. Harada · S. Dunn (✉)
Building 30, Nanotechnology Centre, Cranfield University,
Cranfield MK43 0AL, UK
e-mail: s.c.dunn@cranfield.ac.uk

S. Harada
EPFL–STI–IMX–Ceramics Laboratory,
Building MXC238-Station 12,
CH.-1015 Lausanne, Switzerland

to the problems of segregating phases were addressed and 'simple' one step processes for the hydrothermal synthesis of PZT developed when growing PZT on a surface or, increasingly, as distinct nanoparticles. The current extent of knowledge is limited in that it has largely focused on producing PZT with a stoichiometry that sits on the MPB. If for example, PZT was to be grown using low temperature wet-chemical methods for pyroelectric devices which require a ferroelectric with a lower dielectric constants and loss tangents than those for MEMS applications. Then PZT compositions below the MPB are a better fit for these requirements and hence the ability to adjust stoichiometry can extend the usefulness of this particular synthesis technique. It is for these reasons that we have investigated the development of a low temperature wet-chemical technique that is compatible with producing thing films of substrates. There is however a number of problems that arise when investigating materials that moves towards high zirconia ratios. These are that the reaction rate of zirconia based precursors and zirconia compounds are significantly slower than the equivalent titania materials. As such PZT with high zirconia ratios can be difficult to produce at low temperatures as the products of such reactions tend to be lead or titania rich with excess zirconium remaining as unreacted precursor or unreacted zirconia.

Since the late 1990s there has been significant interest in the use of wet chemical techniques to produce nanoparticles [11]. The development of interest in the growth of nanoparticulate PZT stems from the increased reactivity and, therefore, reduced sintering temperatures of the green part [10] when manufacturing ceramics. There are a variety of methods that are being used to produce these nano structured particles including modified sol-gel type routes [12, 13] as well as coprecipitation [10] and complex precursor techniques. The latter have been utilised to produce particles that range in size from 2 to 200 nm [14–16], and tools developed to investigate the materials at these dimensions [17]. In all these cases a variety of size distributions and morphologies of PZT have been produced but there has been little investigation into the composition changes that are possible with the technique.

The interest in undertaking the work reported in this paper was to synthesise a number of the possible phases of PZT, above and below the MPB, using a low temperature (<160 °C) process. The reduction in processing temperature reduces the overall energy requirements of the process. It also gives an insight into the mechanisms of the growth of the crystals.

2 Experimental methods

To accommodate the high pressures involved in hydrothermal synthesis a commercially available (Parr Instrument Co.), oven heated, acid digestion bomb was used (Model 4744). The device consists of a 45 ml PFTE liner, into which the precursor materials are inserted, surrounded by a screw top steel casing. The absolute maximum rated temperature of the bomb is 250 °C, although when used at temperatures above 200 °C the Teflon liner degrades rapidly. This is because Teflon has a tendency to creep at high pressures making it hard to attain a tight seal (Operating Instructions Parr Acid Digestion Bombs). For this reason hydrothermal experiments were restricted to temperatures at or below 200 °C.

A thermostatically controlled laboratory oven (Memmert) was used to heat the bomb. The oven was pre-heated to the reaction temperature before the start of each experiment. The temperature of the bomb was taken at the surface of the steel casing using a K-type thermocouple and meter accurate to ±0.05 °C. Timing started when the meter recorded the desired reaction temperature. Reaction times were fixed at 4 h. At the end of each experiment the oven was switched off and the door left open to increase the cooling rate of the bomb.

2.1 General hydrothermal procedure for the synthesis of perovskite P(Z)T powder

The basic hydrothermal procedure used in this work was first proposed by Deng et al. [18] for the synthesis of PZT. It is a relatively simple one-step technique that utilises the following precursors in powdered form:

- Lead nitrate—$Pb(NO_3)_2$
- Zirconyl oxychloride—$ZrOCl_2{\cdot}8H_2O$
- Titanium dioxide (anatase)—TiO_2

In their paper, Deng et al. [18] produced 52:48 PZT by adding stoichiometric quantities of the precursors to a home-built autoclave with 100 ml capacity. Next, 80 ml of deionised water were added and the mixture stirred vigorously. Finally, potassium hydroxide flakes were added slowly, with continuous stirring, to give an initial mineraliser concentration of 5 mol/l. After the hydrothermal treatment the powders were filtered and washed with distilled water and ethanol and then dried in an oven at 80 °C. These procedures were replicated exactly during this project. However, since a smaller bomb was used, a scaling factor of 5/16=0.3125 was applied to all the quantities. Table 1 shows the adjusted precursor masses for 52:48 PZT and several other stoichiometries, across the solid solution range, that were attempted in this project. The precursors were mixed with 25 ml deionised water and 7.013 g KOH to reproduce the 5 M initial mineraliser concentration used by Deng et al. [18]. Each stoichiometry was synthesised at least three times to confirm the reproducibility of the results.

Table 1 Hydrothermal precursor masses for stoichiometries across the PZT solid solution.

STOICHIOMETRY→ PRECURSOR↓	$PbTiO_3$ (g)	20:80 (g)	52:48 (g)	60:40 (g)	70:30 (g)	$PbZrO_3$ (g)
$Pb(NO_3)_2$	2.070	2.070	2.070	2.070	2.070	2.070
$ZrOCl_2{\cdot}8H_2O$	–	0.403	1.047	1.208	1.410	2.014
TiO_2	0.499	0.399	0.240	0.200	0.150	–

All chemicals were analytical grade and obtained from Sigma-Aldrich, UK (TiO_2 and KOH) or Fisher Scientific, UK [$ZrOCl_2{\cdot}8H_2O$ and $Pb(NO_3)_2$]. While the precursor materials were not assayed they were used as supplied and were 99.9% certified by the supplier. In all cases the precursor was taken from the same, as supplied, container. A standard Buchner vacuum filtration system was used in conjunction with Whatman No. 6 (3 μm pore size) filter paper, to isolate the product. This trapped the majority of the particles since they had agglomerated after processing. The powders were rinsed using deionised water.

A Siemens D5005 diffractometer was used for all the XRD experiments. The x-ray tube emitted CuK_α (λ= 1.5406 Å) radiation at 40 kV and 30 mA. In general, $\theta-2\theta$ scans were conducted between 20–70° in increments of 0.04° with a dwell time of 1 s per increment. All measurements were made at room temperature. Powder samples were prepared by grinding in a pestle and mortar to limit the possibility of preferential orientation. Phase identification involved matching peaks from a given scan with the accepted values for compounds found in the Powder Diffraction File (PDF-2) database, produced by the International Centre for Diffraction Data (ICDD). The morphology and size distribution of the particles were analysed using an FEI Sirion S-FEG SEM. An FEI Sirion 200 XP FIB system was used to section cubic PZT crystals in order to analyse their internal structure.

3 Results and discussion

In an effort to better understand the hydrothermal reaction mechanism, attempts were made to synthesize PZT stoichiometries on either side of the morphotropic phase boundary (MPB) by altering the Zr/Ti precursor ratio. Figure 1 shows XRD data for powders produced using precursor ratios from 20:80–70:30. Synthesis conditions were identical in each case, with processing temperatures and times fixed at 160 °C and 4 h, respectively. The peaks indexed in Fig. 1 match well to the accepted values for tetragonal 52:48 PZT (PDF card no. 33-0784) and are present in all patterns. The closeness of the resulting XRD pattern and lack of any significant 'bumps' associated with an amorphous phase were used to determine that the expected stoichiometry was produced during the processing. Altering the initial precursor ratio thus appears to have had a limited effect on the resultant PZT phase, as in all cases the XRD pattern produced is that of the MPB phase. Of course, determining whether multiple PZT phases have formed can be difficult, since many of the peaks corresponding to rhombohedral compositions overlap those of tetragonal compositions. What is clear, however, is that under these hydrothermal conditions it has not been possible to produce phase-pure PZT compositions away from the MPB. If an initial precursor ratio of 70:30 had led to the production of rhombohedral 70:30 PZT then we would expect

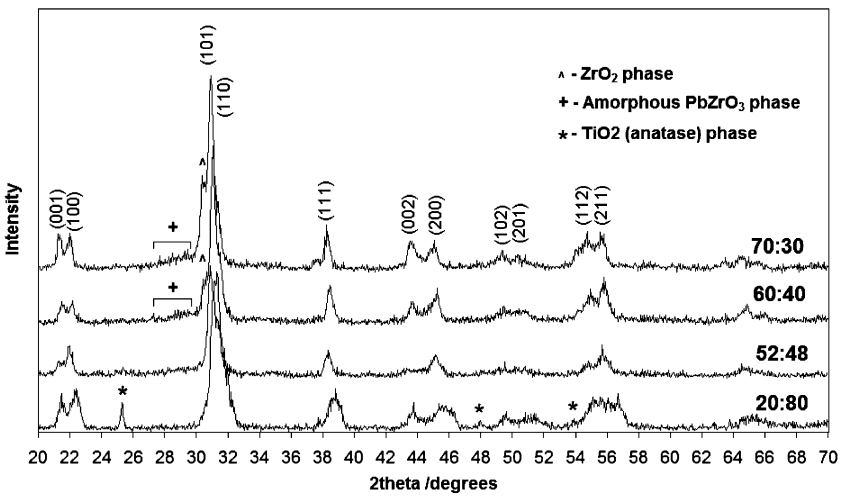

Fig. 1 XRD data for powders synthesised at 160 °C for 4 h from various precursor stoichiometries (indexed peaks correspond to the accepted values for 52:48 PZT, PDF card no. 33-0784)

to see a single (200) peak as opposed to the split (002)–(200) peaks, characteristic of the tetragonal structure. Likewise, a mixture of rhombohedral and tetragonal phases would be characterised by a triplet of peaks in the 42°–47° 2theta range [19]. Instead, we find a strong match to the tetragonal 52:48 composition along with a broad peak attributable to amorphous $PbZrO_3$ and a reflection that can be indexed to ZrO_2 (PDF card no. 41-0017).

A similar situation arose when attempting to synthesise compositions below the MPB. The tetragonality (c/a ratio) of the PZT unit cell is proportional to the Ti content. As such, the separation between split tetragonal peaks in the XRD patterns increases as the Zr content falls. For 20:80 PZT, the accepted lattice constants are: a=3.952 and c=4.151 [20]. Taking the (101)–(110) split peaks as an example, their theoretical 2theta separation for the 20:80 composition should be approximately equal to 0.8°. This level of splitting was not witnessed in the attempted synthesis of 20:80 PZT. What's more, the presence of TiO_2 in the XRD pattern provides further evidence to suggest that the extra titanium has failed to incorporate into the PZT lattice. In summary, the XRD data appears to show that only one PZT phase forms, which lies close to the MPB, regardless of the initial precursor ratio. The subsequent excess of Zr or Ti manifests itself as amorphous $PbZrO_3$ and ZrO_2 above the MPB and TiO_2 below the MPB.

Kutty and Balachandran found that the reaction temperature necessary to synthesise PZT was proportional to the Zr/Ti ratio [21]. In other words, the rhombohedral phase required more energy to form than the tetragonal phase. Attempts to synthesize $PbTiO_3$ (the tetragonal end member of the PZT system) in this investigation have been successful, whereas similar attempts to produce crystalline $PbZrO_3$ have failed (Fig. 2). These results agree with the findings of Kutty and Balachandran and suggest that there was insufficient thermal energy available to form compositions above the MPB. Furthermore, Cheng et al. [22] argued that the formation of PZT was favoured in preference to $PbZrO_3$ and $PbTiO_3$, under the same hydrothermal conditions, due to the greater entropy associated with the PZT system. Their justification for this viewpoint was that an increase in entropy leads to a decrease in the Gibb's free energy of formation of PZT, since $\Delta G=\Delta H-T\Delta S$. This explains why the $PbTiO_3$ phase is absent whenever Zr is present in the precursor solution (Fig. 1).

Incidentally, the hydrothermal $PbTiO_3$ particles, shown in Fig. 2 (inset) had a cubic morphology and in some cases were sub-micron in size. However, the smaller particles were either strongly agglomerated or had grown from a multiple nucleation, as shown by the morphology in Fig. 2.

In a final attempt to synthesise 20:80 PZT, amorphous titania (synthesised via the hydrolysis of titanium isopropoxide) was used as an alternative Ti precursor in place of crystalline anatase. Titania in this form is known to be more reactive [23], so it was hoped that its use could initiate the crystallisation of phases below the MPB. Figure 3 shows the XRD data for a powder synthesised using the amorphous titania precursor. The standard reaction conditions were employed (4 h at 160 °C) and the initial Zr/Ti precursor ratio was 20:80. It can be seen that this, again, resulted in the formation of a PZT phase close to the MPB as opposed to the desired 20:80 phase.

Investigation of the XRD patterns obtained show that no significant amorphous phase is present except in regions above the MPB where we and Deng et al. find amorphous $PbZrO_3$. As the XRD patterns show practically phase pure MPB PZT we do not believe that there is a significant

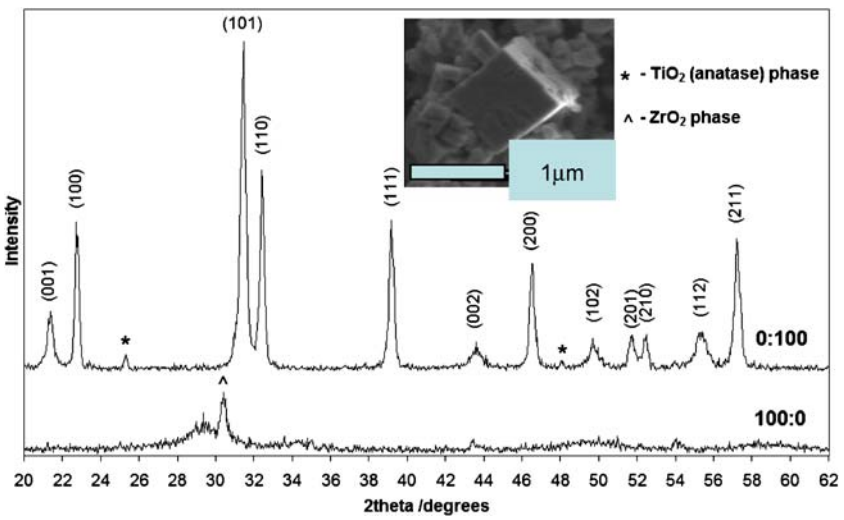

Fig. 2 XRD data for powders synthesised at 160 °C for 4 h with Zr/Ti precursor ratios of 100:0 and 0:100 (indexed peaks correspond to the accepted values for tetragonal $PbTiO_3$, PDF card no. 06-0452). The *inset SEM image* shows the morphology of the $PbTiO_3$ powder

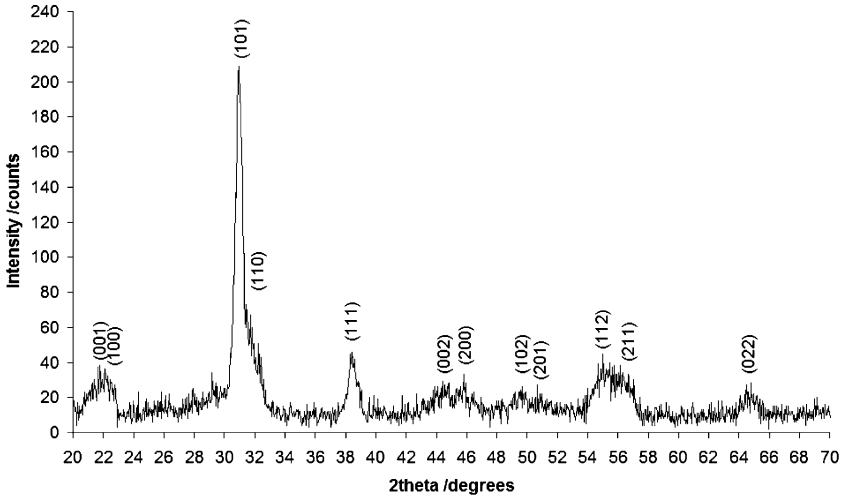

Fig. 3 XRD data for the powder synthesised using an amorphous titania precursor in the Zr/Ti ratio of 20:80 (indexed peaks correspond to the accepted values for 52:48 PZT, PDF card no. 33-0784)

amount of amorphous material being generated in the process. Although we have managed to assign all the peaks in the XRD pattern to known compounds and those not associated with PZT are unreacted TiO_2 we further annealed a small portion (approx. 1 g) of the sample to 900 °C for 4 hours. In order to prevent lead loss the heating was carried out in nested crucibles with a packing powder of 20:80 PZT around the crucible holding the sample of interest. It is known that zirconia precursor materials are slow to react and so to discount the possibility of unreacted precursors being present in an amorphous form the heat treatment was conducted. The results of this further anneal are shown in the XRD pattern of Fig. 4. The XRD pattern after annealing is very similar to that produced from the as-prepared samples. The only change that is observable is a slight broadening of the peaks around 31° and 44° 2theta, which could be associated with the development of $PbTiO_3$. This we believe is a reaction between a small fraction of unreacted PbO and titanium precursors. The lack of significant changes in the two XRD patterns (Figs. 3 and 4) gives further evidence that the hydrothermal process has left no amorphous material that is evident within the detection limits of the XRD system used.

The morphology of the powder synthesised using the amorphous titania precursor was varied. It was predominantly composed of micron-sized cubic crystals [Fig. 5(a)] that were smaller than those seen during equivalent experiments where crystalline anatase was used as a Ti source. Unfortunately the crystals agglomerated into large masses that also contained amorphous or partially crystallised material. Other morphologies were seen including circular platelets [Fig. 5(b)]. These variations are most probably due to inhomogenieties in the precursor mixture. The hydrous titania gel platelets could be the same as those found in the low temperature hydrothermal synthesis of lead titanate ($PbTiO_3$) particles using tetramethylammonium hydroxide [24].

4 The effects of $Pb(NO_3)_2$ precursor concentration

Experiments were conducted to determine the effects of Pb precursor concentration on the formation of PZT in the

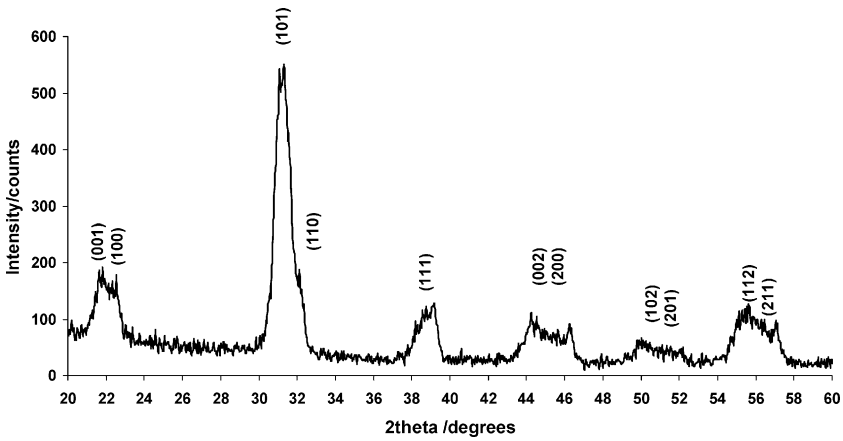

Fig. 4 XRD data for the powder synthesised using an amorphous titania precursor in the Zr/Ti ratio of 20:80 and annealed at 900 °C for 4 h (indexed peaks correspond to the accepted values for 52:48 PZT, PDF card no. 33-0784)

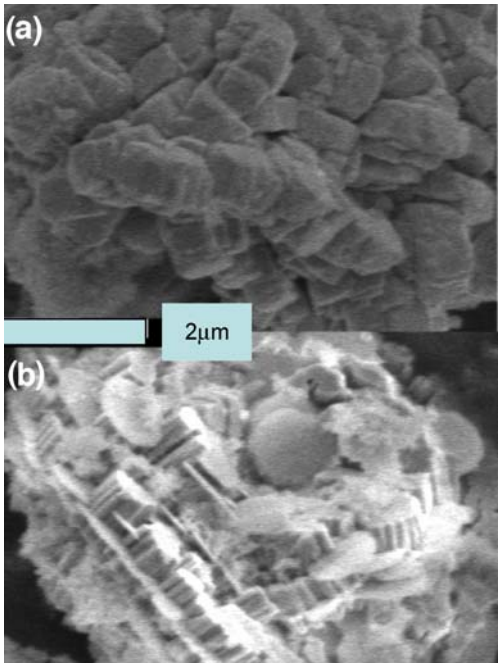

Fig. 5 SEM images showing two types of particle morphology observed after substituting crystalline anatase with amorphous titania in the attempted hydrothermal synthesis of 20:80 PZT: (**a**) agglomerated micron-sized cubes and (**b**) circular platelets

general hydrothermal reaction. It was found that a 100% Pb $(NO_3)_2$ excess produced unagglomerated PZT particles with a cubic morphology under the standard synthesis conditions of 4 h processing at 160 °C (Fig. 6). The particles were well faceted and little amorphous/unreacted material remained after processing, in contrast to previous experiments conducted without Pb-excess. Multiple nucleation was also observed in some cases, as was the precipitation of crystallised particles in close proximity to the precursor gel (Fig. 7). The average size of the particles was around 5 μm. During the early stages of the hydrothermal reaction Pb ions play an important role in infiltrating and helping to dissolve the coprecipitated Zr–Ti gel. As PZT crystals precipitate the Pb ion concentration in solution starts to fall, hence reducing the rate of dissolution. An excess of Pb

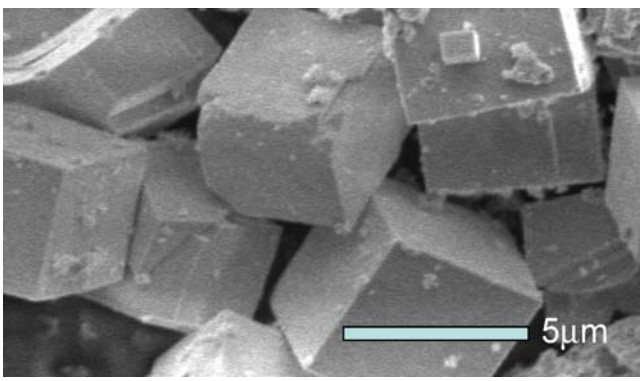

Fig. 6 SEM image of PZT particles produced using a 100% Pb precursor excess

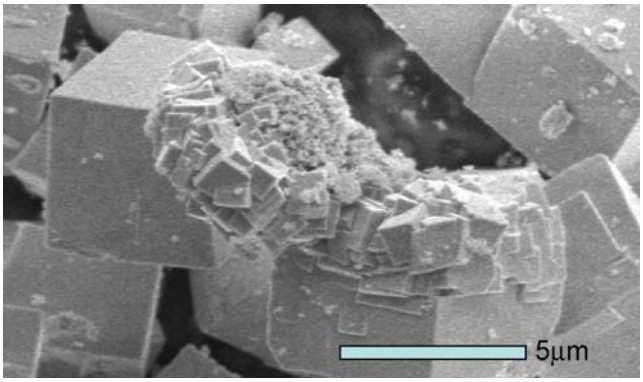

Fig. 7 SEM image showing twinning and the precipitation of crystals near to the precursor gel

precursor compensates for this deficiency and ensures more complete dissolution of the gel.

FIB milling of PZT crystals produced using a 100% Pb precursor excess showed a dense, almost homogeneous internal structure in comparison to crystals synthesised without a Pb excess (Fig. 8). This evidence would suggest that a Pb-excess helps to improve crystallisation during the precipitation phase.

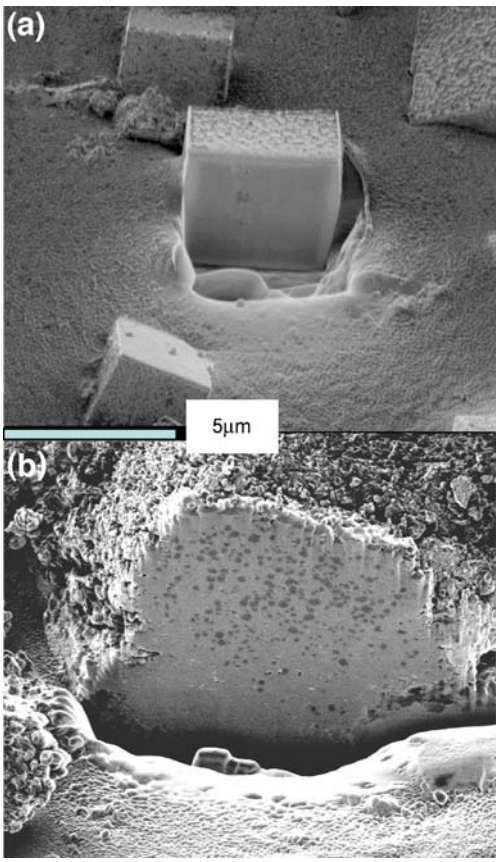

Fig. 8 FIB images of PZT crystals synthesised (**a**) with and (**b**) without a Pb-excess and subsequently sectioned using FIB milling. Note the greater degree of crystallisation exhibited by the crystal processed using a Pb excess

5 Conclusions

The main conclusion that can be drawn from this work is that the relationship between the precursors and processing conditions can have a major impact on the resultant phase, and morphology of the produced material. Differences in reactivity between the precursors ensure that there are differences in the final ratio of Ti and Zr in the PZT and that they do not follow the precursor ratios. Addition of excess Pb precursor can assist in the production of high quality crystals by aiding the dissolution of the Zr–Ti gel. The inability to make phases away from the MPB at the processing temperatures employed highlight the difficulty in producing a variety of PZT phases when starting from separate Ti and Zr precursors. Instead, a phase close to the MPB is produced whilst the excess precursors fail to incorporate into the PZT lattice.

References

1. S.S. Roy, H. Gleeson, C.P. Shaw, R.W. Whatmore, Z. Huang, Q. Zhang, S. Dunn, Integr. Ferroelectr. **29**, 189 (2000)
2. S. Dunn, R.W. Whatmore, J. Euro. Ceram. Soc. **22**(6), 825–833 (2002)
3. S. Dunn, A.P. De Kroon, R.W. Whatmore, J. Mater. Sci. Lett. **20**, 179 (2001)
4. Z. Huang, Q. Zhang, R.W. Whatmore, J. Appl. Phys. **85**, 7355 (1999)
5. S. Dunn, J. Appl. Phys. **94**(9), 5964–5968 (2003)
6. T. Morita, T. Kanda, Y. Yamagata, M. Kurosawa, T. Higuchi, Jpn. J. Appl. Phys. **36**, 2998 (1997)
7. B. Su, C.B. Ponton, T.W. Button, J. Euro. Ceram. Soc. **21**, 1539 (2001)
8. J. Zeng, M. Zhang, Z. Song, L. Wang, J. Li, K. Li, C. Lin, Appl. Surface Sci. **148**, 137 (1999)
9. T. Morita, Y. Cho, Appl Phys Lett. **85**, 2331 (2004)
10. J.-H. Choy, Y.-S, Han, J.-T, Kim, J. Mater. Chem. **5**, 65(1995)
11. R.N. Das, P. Pramanik, Mater. Lett. **40**, 251 (1999)
12. Y. Faheem, M. Shoaib, J. Am. Ceram. Soc. **89**, 2034 (2006)
13. S. Linardos, Q. Zhang, J.R. Alcock, J. Europ. Ceram. Soc. **26**, 117 (2006)
14. R.N. Das, R.K. Pati, P. Pramanik, Mater. Lett. **45**, 350 (2000)
15. P. Pramanik, R.N. Das, Mater. Sci. Eng. **A304–A306**, 775 (2001)
16. S. Bose, A. Banerjee, J. Am. Ceram. Soc. **87**, 487 (2004)
17. S. Dunn, C.P. Shaw, Z. Huang, R.W. Whatmore, Nanotechnology, **13**(4), 456–459 (2002)
18. Y. Deng, L. Liu, Y. Cheng, C.-W. Nan, S.-J. Zhao, Mater. Lett. **57**, 1675 (2003)
19. A. Boutarfaia, S.E. Bouaoud, Ceram. Int. **22**, 281 (1996)
20. S. Fushimi, T. Ikeda, J Am. Ceram. Soc. **50**, 129 (1967)
21. T.R.N. Kutty, R. Balachandran, Mat. Res. Bull. **19**, 1479 (1984)
22. H. Cheng, J. Ma, B. Zhu, Y. Cui, J. Am. Ceram. Soc. **76**, 625 (1993)
23. M.M. Lencka, A. Anderko, R.E. Riman, J. Am. Ceram. Soc. **78**, 2609 (1995)
24. S-B. Cho, J-S. Noh, M.M. Lencka, R.E. Riman, J. Euro. Ceram. Soc. **23**, 2323 (2003)